energies

MDPI

Article

Distributed Volt-Var Curve Optimization Using a Cellular Computational Network Representation of an Electric Power Distribution System

Hasala Dharmawardena [1] and Ganesh Kumar Venayagamoorthy [1,2,*]

[1] Real-Time Power and Intelligent Systems Laboratory, Holcombe Department of Electrical and Computer Engineering, Clemson University, Clemson, SC 29634, USA; hasala@ieee.org
[2] School of Engineering, University of KwaZulu-Natal, Durban 4001, South Africa
* Correspondence: gvenaya@clemson.edu

Abstract: Voltage control in modern electric power distribution systems has become challenging due to the increasing penetration of distributed energy resources (DER). The current state-of-the-art voltage control is based on static/pre-determined DER volt-var curves. Static volt-var curves do not provide sufficient flexibility to address the temporal and spatial aspects of the voltage control problem in a power system with a large number of DER. This paper presents a simple, scalable, and robust distributed optimization framework (DOF) for optimizing voltage control. The proposed framework allows for data-driven distributed voltage optimization in a power distribution system. This method enhances voltage control by optimizing volt-var curve parameters of inverters in a distributed manner based on a cellular computational network (CCN) representation of the power distribution system. The cellular optimization approach enables the system-wide optimization. The cells to be optimized may be prioritized and two methods namely, graph and impact-based methods, are studied. The impact-based method requires extra initial computational efforts but thereafter provides better computational throughput than the graph-based method. The DOF is illustrated on a modified standard distribution test case with several DERs. The results from the test case demonstrate that the DOF based volt-var optimization results in consistently better performance than the state-of-the-art volt-var control.

Keywords: cellular computational networks; distributed energy resources; optimization; photovoltaics; power distribution system; voltage control

Citation: Dharmawardena, H.; Kumar Venayagamoorthy, G. Distributed Volt-Var Curve Optimization Using a Cellular Computational Network Representation of an Electric Power Distribution System. *Energies* **2022**, *15*, 4438. https://doi.org/10.3390/en15124438

Academic Editor: Abu-Siada Ahmed

Received: 15 April 2022
Accepted: 30 May 2022
Published: 18 June 2022

1. Introduction

The electric power system is undergoing a rapid transition from a fossil fuel-based, central system to a renewable distributed energy resource-based distributed system due to the need to enhance the security of supply, reduce cost, enhance sustainability, and battle climate change [1]. The bulk of this transformation is a result of the rise of the prosumager, a consumer that also produces and stores energy [2]. All consumers who have installed distributed energy resources such as solar PV and storage are prosumagers, and they are at the center of the energy transition. A bulk of the prosumagers are connected to the power distribution system. Unfortunately, the distribution grid infrastructure has been one of the most neglected infrastructures worldwide. It is the least prepared to serve the rapidly transforming needs of the energy sector. For example, in some places in the United States, the average age for the distribution of assets are between fifty to seventy years, thus past the expected lifetime of thirty years [3].

Climate change combined with digitization has accelerated the decarbonization of the energy sector, causing rapid electrification of multiple facets of human society [4]. The quality of life and the functioning of society at large is increasing in dependency on electricity. The distribution grid is at the epicenter of transformation. Therefore, while there has been weak historic investment in the distribution grid, the highest level of quality of service, resilience, and reliability is required at the distribution grid. For example, it is critical to maintain a high-quality voltage profile, at all times because of the sensitivity of the customer equipment, regulatory requirements, as well as financial requirements to minimize losses in the distribution grid [5]. The need for performance is the highest at the weakest link of the power system.

The multi-directional power flow needs to be supported by an aging distribution infrastructure initially designed for unidirectional power flow, which further escalates the complexity of the problem. The stress on the distribution system and the need to improve the quality of service delivered at the distribution system have increased simultaneously, highlighting the need to address both of these challenges. Developing technologies will hasten the energy sector's transition towards a sustainable, cost-efficient, and secure future.

It is increasingly clear that ensuring voltage quality is one of the distribution system's most significant challenges. The main drivers of this voltage control challenge are the multi-directional power flow from intermittent generation and new loads with considerable magnitude and low diversity, such as Electric Vehicles. Voltage control is implemented using regulators and capacitor banks in a traditional distribution system. Since the conventional distribution system consists of unidirectional, top-down power flow with slow changes in demand, this method can be effectively used to regulate voltage in a traditional distribution grid. However, with the rise of the prosumagers, where solar PV dominates production, the variability of solar irradiation causes significant fluctuations in the power flow resulting in a degraded voltage profile [6]. Unfortunately, traditional voltage regulators are not fast enough to counter this problem since they depend on slow devices such as mechanical tap changers [7]. Furthermore, the cost associated with an increasing number of tap changing will be significant to the operator due to the degradation of the equipment lifetime.

1.1. Optimization

Optimization can be executed in numerous ways. The classification of optimization based on framework, implementation, objective function, and solution is shown in Figure 1 and described below.

- *Centralized versus Decentralized:* The framework for optimization is centralized if data from all the nodes/buses are communicated to a central point; on the other hand, it is decentralized if the data are consumed locally. Therefore, both communication and sensing are limited to the local node.
- *System versus Cell versus Node:* An objective function can be formulated in many ways. This formulation (for a N node system) can be for system-wide optimization (all nodes), cell-wide (a set of nodes/sub-system), or node optimization (local optimization).
  - System-wide optimization (one objective function for the system) is executed in a centralized or decentralized manner. The ideal approach is to run it in a centralized way. A decentralized approach does not guarantee a system-wide global optimal solution.
  - Node optimization (N Objective functions), where each node has a unique objective function, can be executed in a centralized or decentralized manner. The best approach is a decentralized execution. A centralized approach does not guarantee a node-level optimal solution.
  - Cell-wide optimization (between 1 and N objective functions) refers to having one objective function per cell (sub-system). This is a decentralized approach, but decentralization is lower than node optimization.
- *Global versus Local:* During any optimization, based on the problem being optimized, there could be multiple local minima and a global minimum. Local optimization seeks to find the local minimum appropriate in a local search space. Global optimization seeks to find the lowest minimum of all local minima in a global search space.

- *Sequential versus Parallel:* The optimization implementation is sequential if executed in a sequential computing environment using a sequential algorithm. If performed in a distributed environment using a parallel computing platform, it is parallel.

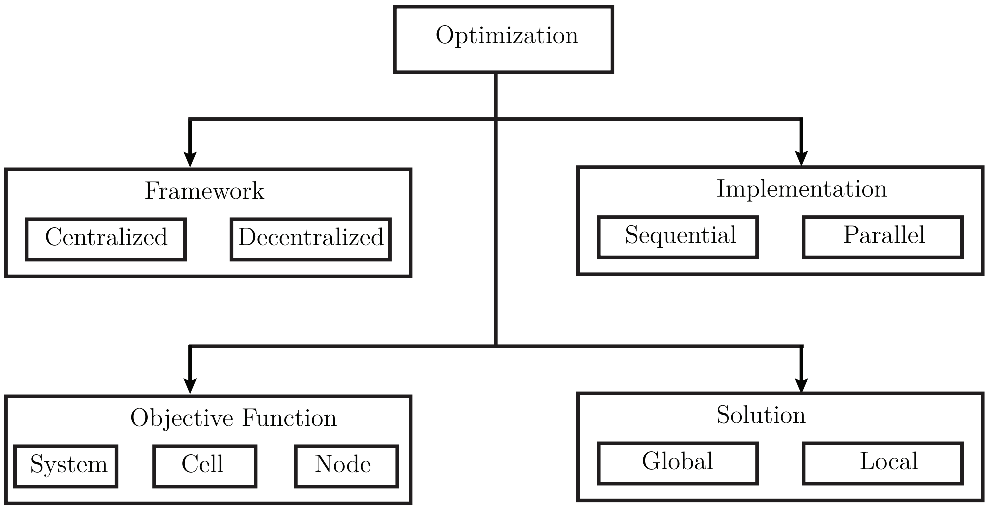

Figure 1. The classification of optimization based on framework, implementation, objective function, and solution.

Different combinations of these approaches can be selected to satisfy the requirements of an application. A distributed optimization framework is advantageous when a system-wide optimization is sought while not having access to all data at a central location. The DOF allows for decomposing the objective function at the system-level into a number of objective functions that can be solved independently seeking a global optimal solution.

1.2. State of the Art

The distribution system operators solved the voltage quality challenges of the distribution system by installing tap changers and capacitor banks. Whereas these conventional solutions are still in use, the modern state-of-the-art solutions are centered around power electronics devices such as d-statcom [8], edge of network grid optimizer [9], and dynamic voltage restorer [10]. However, these components are costly to install and maintain while needing support infrastructure that might not even be available to the DSO.

Instead of installing additional devices, this study navigates the possibility of optimally leveraging the flexibility of using the prosumager owned electronic power inverter to control the distribution system voltage. This study assumes that the inverter's idling reactive power capacity is available to support voltage control [11]. The prosumagers can be compensated for this ancillary service.

All optimization variants rooted in a centralized framework operate where a central unit will process the measurements, perform necessary computation, and dispatch the appropriate operation set-points to a local controller. The local controller controls the prosumager. Each local node needs to be directly connected to the central controller. The advantage of this approach is that the central controller will have access to local measurements. Therefore, assuming perfect optimization, it has the potential to operate at global optimality. The disadvantage of this approach is that the central controller will have to process multiple input and output data streams and solve for a large number of variables. This approach can be applied for both real-time control [12] and optimal power flow based operation [13–15]. Efforts to optimize the local reactive power control over a lengthy time horizon have also been presented in the past [16]. However, the large magnitude of optimization parameters and difficulty producing granular forecasts at the required accuracy make the central approach infeasible for most use-cases. Additionally, a failure in the communication link or the central controller would result in catastrophic failure, pointing to reliability challenges associated with these single points of failure.

Therefore, this approach is not robust nor scalable and is constrained by the requirement to communicate large amounts of data and optimize at high speeds. Consequently, this approach comes with untenable implementation challenges.

All optimization variants rooted in a decentralized framework rely only on local measurements. Each node in the system will have its unique, and decisions will be taken only based on local measurements. Therefore, this does not require computation and optimization on large data sets or communication infrastructure. Consequently, local optimization is robust. However, since the local optimizer is only aware of its local environment, the results will likely be sub-optimal. This method has been extensively analyzed [6,17] and forms the basis for the widely implemented state of the art voltage control defined in the IEEE 1547-2018 standard [18]. However, since it is a local framework, the synergies of the connected resources will not be leveraged to gain local and global optimization, and the contributions will be highly skewed based on the spatial distribution of the prosumers in the distribution feeder.

For example, in the distributed optimization framework presented in this paper, there is limited communication between nodes, and optimization is executed across a sub-set of the nodes. Similar approaches have been investigated in recent studies such as [19–21]. However, these approaches do not have a cell-wide objective function. Therefore, the number of iterations required for each solution, the assumptions for system modeling, and the constraints on the maximum possible prosumers limit their applicability.

1.3. Contributions

This paper proposes a method to optimize multiple volt-var curves of DERs in a power distribution system with distributed cell-based optimization to address the challenges mentioned above. The current state of art optimizes the volt-var curves over a long time horizon, but the optimization is not able to address the temporal dynamics in a minutes time frame [22]. Additionally, the state-of-the-art approaches are based on central optimization [23], which limits the applicability of such a method [24] in many practical systems. The proposed enhances the flexibility of operation by considering the spatial and temporal dynamics of the distribution system and optimizing the system in a granular, distributed manner. This will utilize the complete flexibility of the DERs to support the system operations in a distributed manner. The uniqueness of the proposed approach is that it allows for decentralized and distributed optimization of distribution systems with significant penetration of distributed energy resources. The main contributions of this paper are:

- A scalable distributed optimization framework has been developed for concurrent multiple volt-var curve optimization. This method is based on creating a cellular computation network representation of the electric power distribution system with DERs, which allows for distributed data-driven modeling and optimization of the distribution system.
- A ranking method for cell prioritization for optimization has been developed. Cell prioritization for optimization based on a formulated impact ranking criteria improves the computational throughout for determining optimal volt-var curve parameters. Two methods, namely, graph and impact-based methods, are studied.
- The application of DOF on a modified IEEE 34 bus test system with 100% DER penetration has been illustrated. The operational results obtained with volt-var curves optimized using the DOF consistently outperforms those obtained state-of-the-art volt-var curves.

The study is organized as follows: Section 2 formulates the problem statement, Section 3 describes the framework for distributed VVC optimization, and Section 4 describes the simulations used to demonstrate the framework. Section 5 shares the results, as well as the insights attained through the results. Section 6 concludes the study.

2. Problem Formulation

Given a power distribution system with N nodes/buses the net power injection at bus i, $S_{inj,i}$, is given by

$$S_{inj,i} = S_{inv,i} - S_{dem,i} = f_i(V, \delta) \tag{1}$$

where $S_{inv,i} = (P_{inv,i} + jQ_{inv,i})$ represents inverter power injection at bus i and $S_{dem,i} = (P_{dem,i} + jQ_{dem,i})$ represents load power consumption at bus i. P, Q, denote active power and reactive power, respectively. V and δ represent the vector of all node voltage magnitudes and voltage angles. The N simultaneous equations generated by applying (1) for all N nodes define the power flow of the system. The droop function at the bus i, g_i, which defines the inverter reactive power dispatch at time, $t + \Delta t$, is written as

$$Q_{inv,i}(t + \Delta t) = g_i(V_i(t)) \tag{2}$$

$$\begin{aligned} V_2 &= V_1 + dV_1 \\ V_3 &= V_2 + dV_2 \\ V_4 &= V_3 + dV_3 \end{aligned} \tag{3}$$

The function g_i is the piece-wise linear curve shown in Figure 2 and defined below. The controllable variable for one inverter, x_i, has a dimension of six as given in (4). The vector x_i defines the VVC of the node i:

$$g_i(V_i) = \begin{cases} Q_1 & V_i \leq V_1 \\ -\dfrac{Q_1}{V_2 - V_1}(V_i - V_2) & V_1 < V_i \leq V_2 \\ 0 & V_2 < V_i \leq V_3 \\ \dfrac{Q_2}{V_4 - V_3}(V_i - V_3) & V_3 < V_i \leq V_4 \\ Q_2 & V_1 \leq V_i \end{cases}$$

$$x_i = \{Q_{i,1}, Q_{i,2}, V_{i,1}, dV_{i,1}, dV_{i,2}, dV_{i,3}\} \tag{4}$$

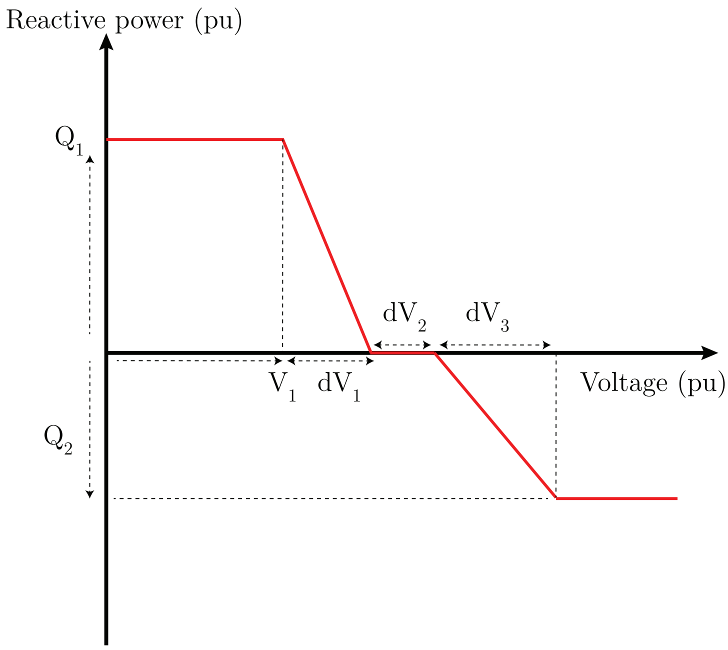

Figure 2. The volt-var curve as defined in the IEEE 1547 standard. The curve is optimized by changing the six variables shown on this plot. The x-values of the VVC is given by (3).

The optimization problem is formulated as follows:

$$\min_{\mathbf{x}\in S} U_{sys} = \frac{1}{T}\sum_{i=1}^{T}(\frac{1}{N}\sum_{i=1}^{N}(V_i - V_{rated,i})^2)^{0.5} \tag{5}$$

subject to the constraints given by (6). These constraints need to be defined in such a way to ensure that the resulting volt-var curves are realistic, based on [25]. Whereas voltage optimization is the objective of this study, it is possible to use any other utility function interest, for example, line losses.

$V_{rated,i}$ is the ideal value for voltage magnitude at node i and T is the time period, S is the solution space of the problem. The overall goal is to optimize voltage quality over a time period T. Therefore, the average root mean squared value of the voltage magnitude difference from the ideal voltage, defined in (5), was chosen as the objective function:

$$\begin{aligned} Q_{1,min} &< Q_{i,1} < Q_{1,max} \\ Q_{2,max} &< Q_{i,2} < Q_{2,max} \\ V_{1,min} &< V_{i,1} < V_{1,max} \\ dV_{1,min} &< dV_{i,1} < dV_{1,max} \\ dV_{2,min} &< dV_{i,2} < dV_{2,max} \\ dV_{3,min} &< dV_{i,3} < dV_{3,max} \end{aligned} \tag{6}$$

The optimal solution, $\mathbf{x}$, is a $N \times 6$ matrix and takes the form given in (7).

$$\mathbf{x} = \begin{pmatrix} x_1 \\ \vdots \\ x_i \\ \vdots \\ x_N \end{pmatrix} = \begin{pmatrix} Q_{1,1} & Q_{1,2} & V_{1,1} & dV_{1,1} & dV_{1,2} & dV_{1,3} \\ \vdots & \vdots & \ddots & \vdots & & \\ Q_{i,1} & Q_{i,2} & V_{i,1} & dV_{i,1} & dV_{i,2} & dV_{i,3} \\ \vdots & \vdots & \ddots & \vdots & & \\ Q_{N,1} & Q_{N,2} & V_{N,1} & dV_{N,1} & dV_{N,2} & dV_{N,3} \end{pmatrix} \tag{7}$$

3. Distributed Optimization Framework

The structural overview of the framework is shown in Figure 3. The developed implementation of the DOF has a decentralized execution, cell-wide objective function formulation, a global solution, and is implemented sequentially.

In the first step of the proposed framework, the CCN representation of the EPDS is developed based on [26]. Next, the CCN representation is used for distributed optimization based on three structural levels: node, cell, and system. The inverter devices are physically located at the nodes, and they contribute to the distributed optimization by sharing local measurements with the cell level operator and by adapting the volt-var curves based on cell operator signals.

The optimal volt-var curves for all nodes are evaluated at the cell level of the distributed optimization process. The utility function for optimization is limited to local optimization, and, therefore, the optimization variables are the set of x vectors for local volt-var curves. The system-level iterative optimization algorithm uses the CCN representation to drive cell optimization.

3.1. CCN Representation of the EPDS

The developed framework optimizes the volt-var curve of the inverters connected to the power distribution system, using the CCN representation of the EPDS in a distributed manner. In general, a cellular computational network consists of interconnected cells that interact with each other to realize a common goal. This approach has been used for distributed modeling, optimization, and control of power systems [27,28] in the past. This study utilizes the cellular computational network representation for a power distribution system that was developed in [26] and applies it for distributed optimization of voltage control. The main advantage of this approach in comparison to other methods such as [16,20] is that it allows for the collection of nodes into a cell structure for efficient distributed optimization across a near-future time horizon. Based on available computational resources and the design goals, the designer has the flexibility in deciding on the level of optimization that needs to be carried out.

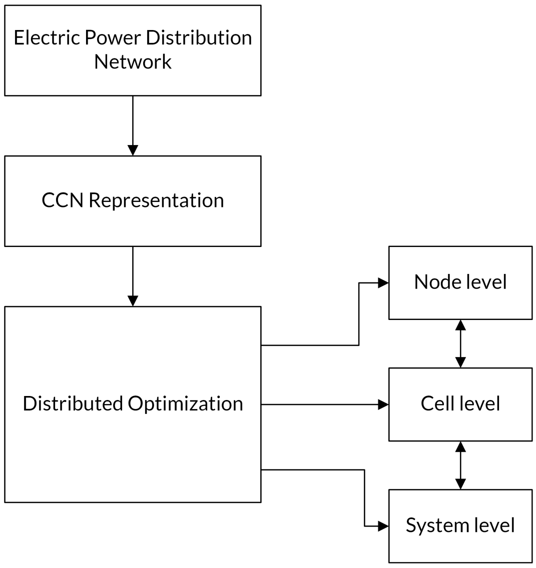

Figure 3. Overview of the proposed DOF.

3.2. Node Level Control

The overview of the node-level control is shown in Figure 4. In this method, the state-of-the-art VVC is extended by appending the ability to change the volt-var curve parameters dynamically. Therefore, the parameters of the volt-var curve (x) are an external input to the inverter controller. The external information is provided by the cell-level optimization function and requires a communication channel. The distribution system modeling method presented in [26] is used in the selection of the cells to form the CCN representation. Since the DOF additionally requires modeling of the impact of the DER, ref. [26] is extended to include DER control.

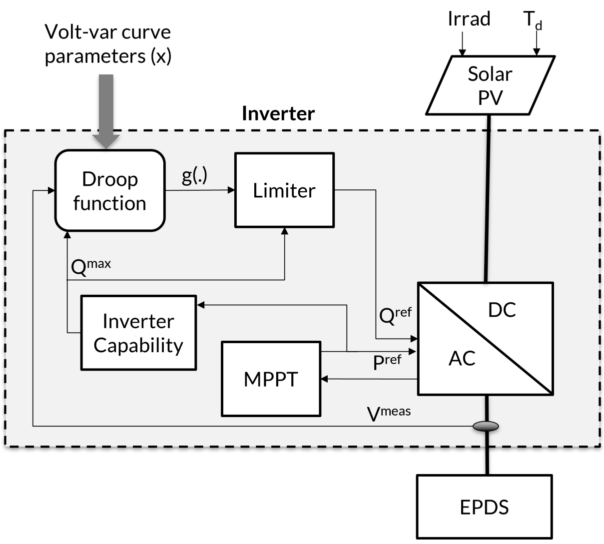

Figure 4. The overview of the prosumer based PV inverter control system. The volt-var curve parameters (x) is changed by the cell operator. This is the node level optimization of the DOF.

Der Modeling

The model applied for DERs in this study assumes that the consumer generation is based on solar PV plants. As described in the introduction, solar PV is the dominant DER in distribution systems, and it is expected to grow exponentially in the next few decades. If the primary energy source is changes from PV, it is still possible to use the presented approach to model any other DER by changing the generation model.

The source of energy is solar radiation which the PV cells convert to electricity [29]. Based on the PV characteristics, the maximum power DC power output from the PV plant at time t, $P_{DC(t)}$, can be determined by (8). Here, $P_{pv,rated}$ is the maximum power from the PV array, $Irrad(t)$ is the irradiation level at time t, and $T_d(t)$ is the temperature derating factor from the power temperature characteristic curve. Here, P_{DC} is assumed to vary linearly with irradiation:

$$P_{DC}(t) = P_{pv,rated} \times Irrad(t) \times T_d(t) \tag{8}$$

The model of the inverter is given in Figure 4. Typically, the power setpoint for the inverter is based on an MPPT algorithm. For the time step of interest, it is assumed that MPPT based reference value is equal to P_{ref}. The setpoint for reactive power, Q_{ref}, is determined based on the control loop shown in Figure 4. The Q_{ref} is determined based on the inverter capability curve, the user selected priority (operation) mode (active power or reactive power priority), and the droop function (volt-var curve).

Assuming the only inverter capability constraint is current carrying capacity and inverter reactive power priority operation mode, the maximum reactive power that is available for dispatch, Q_{max}, is given by

$$Q_{max} = \sqrt{(S_{max})^2 - (P_{ref})^2} \tag{9}$$

The value of Q_{max} is an input to the limiter function, and it changes with solar irradiance. The function g, which defines the volt-var characteristics of the active DER, shown in Figure 2 has six independent parameters. The first two parameters define the maximum reactive power contribution (y-axis), and the last four determine the voltage for the reactive power contributions. The limiter considers the constraints and user-selected operation mode and provides the setpoints to the power electronic converter.

3.3. Cell Optimization

The algorithm used for the optimization of cell k is shown in Figure 5. An optimizer optimizes the selected cell. A time-series simulation that uses both the system model and expected operational data serves as an input to the optimizer. The operational data, the data set of independent load flow variables (loads and generation) for the optimized time window T, could be a near-future forecast [30], a sliding window average forecast [31], or a persistent forecast [32]. A near-future forecast is better than a sliding window average forecast, which is better than a persistent forecast. A better forecast allows for better results in operation.

The objective function for the optimization is the cell utility (U_{cell}). U_{cell} takes into account the set of internal cell voltages and the boundary node voltage of the neighboring cells. The cell utility function, U_{cell}, is the root mean squared voltage and is given by (10). Here, m includes nodes belonging to cell k and the immediate neighbor nodes of cell k. The optimizer computes the best possible set of optimization variables for the cell, $x_{cell}(k)$. This value is then updated in the system model. The system will then operate with the optimal volt-var curve based on the results from the last optimization cycle till a new optimization is carried out, and the values are updated for the next siding window of data. Therefore, the data used for optimization is different from the data used to operate the system. The sub-optimality arises from the difference between the system state that it was optimized for and the actual system state, which could be minimized by using an improved near future forecast or optimizing at a shorter time interval:

$$U_{cell} = \frac{1}{T}\sum_{i=1}^{T}(\frac{1}{m}\sum_{i=1}^{m}(V_i(\mathbf{x}) - V_{rated})^2)^{0.5} \tag{10}$$

If a hypothetical distribution system consists of n cells, each of which has equal m number of volt-var curves, central optimization will require $n \times m \times 6$ variables to be optimized. However, the proposed distributed approach will only need $m \times 6$ parameters to be concurrently optimized. Therefore, the DOF significantly decreases the dimension of the optimization problem. The cell optimizer could be placed on a computing platform in the distribution system control center or placed on multiple spatially separated physical devices.

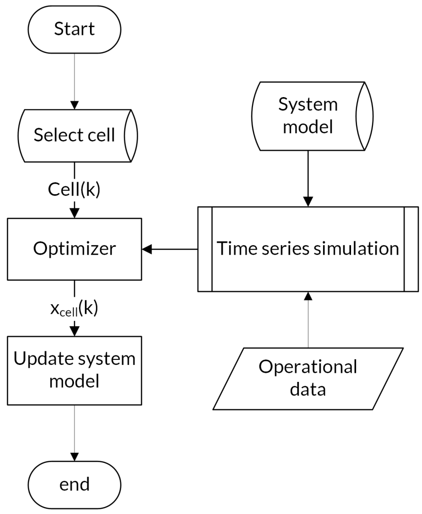

Figure 5. The implemented algorithm for cell level optimization.

3.4. System Optimization

The system-level optimization is carried out by iteratively optimizing the cells. The priority for selecting cells for system optimization is based on an index defined as the cell rank, from the lowest to the highest CR. Two approaches for choosing the cell rank are presented in this study. The algorithm used for the optimization of cell k is shown in Figure 6. The first step for system optimization is to develop the CR table. This provides the sequential order for cell optimization. Next, cell-level optimization of the cell with the current lowest priority (of non-optimized cells) is carried out. In the next step, the system objective function, U_{sys}, is evaluated, and a decision is made to iterate again or to stop the system optimization based on the stop criteria. The stop criteria for system optimization are either reaching maximum cell iterations or the required minimum value for system utility.

3.4.1. Graph Based Cell Rank Evaluation

In the graph-based approach, the cell rank (CR) is based on the graph structure of the CCN. The topology is processed, and the CR is given based on the tree traversal order from the furthermost leaf cell to the root, covering every cell in the graph. The furthermost leaf cell is given the lowest CR and will have the highest priority in system optimization. This approach is simple and only requires topology information.

3.4.2. Impact Based Cell Rank Evaluation

The objective of proposing the impact factor-based approach is to increase the performance of the iterative optimization. In this approach, the CR is based on a calculated impact factor that considers the ability of any cell to contribute to the optimization of the system voltage. The impact factor evaluates the combined effect of the system voltage sensitivity to reactive power and the reactive power injection capability of a cell. The first cell to be optimized is the cell that has both a high sensitivity to the system utility and a large reactive power injection resource.

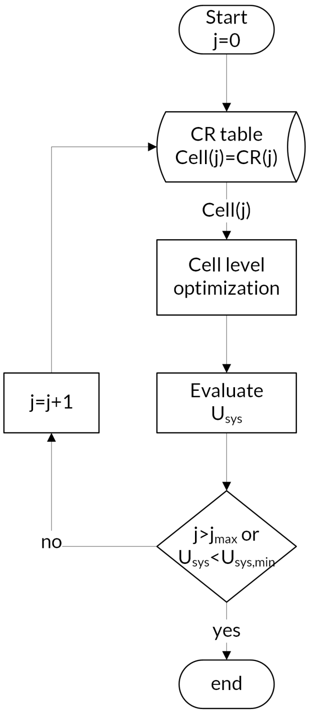

Figure 6. The implemented algorithm for system level optimization.

The first step in the process is to find each cell's total apparent power capability. Next, the available reactive and active power are assembled to create a cellular virtual power plant representation. Each cell has a virtual reactive (Q_{cell}) and active power load and generation. This step requires central information gathering and is used only to prioritize the optimization. Next, an artificial reactive power generation of δQ is injected into each cell. The δQ is distributed across the nodes proportional to the installed capacity of the generation. The U_{sys} sensitivity to this δQ is next evaluated by running an independent power flow and calculating the $\frac{\partial U_{sys}}{\partial Q_{cell}}$ value of each cell. The impact factor (IF) of all the cells is then calculated by using (11). If the operating system point changes significantly, then a new impact factor calculation needs to be carried out since the impact factor is dependent on the power flow Jacobian, and the power flow Jacobian varies with the operating point:

$$IF = Q_{cell} \cdot \frac{\partial U_{sys}}{\partial Q_{cell}} \tag{11}$$

4. Case Study

The case study is based on a modified IEEE 34 distribution system given in Figure 7. It is a medium-sized long radial distribution system that originally existed in Arizona and had voltage control challenges due to its length. The system has 95 nodes and 68 loads. This system was modified by adding 28 PV inverters shown in Table A2. The system includes twenty-two three-phase PVs and eight single-phase PVs distributed across the feeder. The active power generation is limited to the load active power consumption. Therefore, this modified test case describes a system with approximately 100% DER penetration. The solar inverters are assumed to be rated for 120% of the rating of the connected PV. The blue boxes show the cell boundaries of the cellular computation design. The inter-cell power flows and the cell-to-cell physical connections are shown in red and green. The irradiance curves are assigned to ensure the spatial correlation of solar irradiation and are based on four solar irradiation curves for the PVs given by Figure 8. The loads are all set to four time-varying, and unique load curves are shown in Figure 9. The loadshapes are assigned randomly to the loads. They are based on load time series data extracted from [33]. The PV irradiation shapes are assigned based on spatial information. A Particle Swarm Optimization [34] based optimizer is selected for the cell optimization. In the case study, it was assumed that the ideal voltage for each of the nodes is 1 pu.

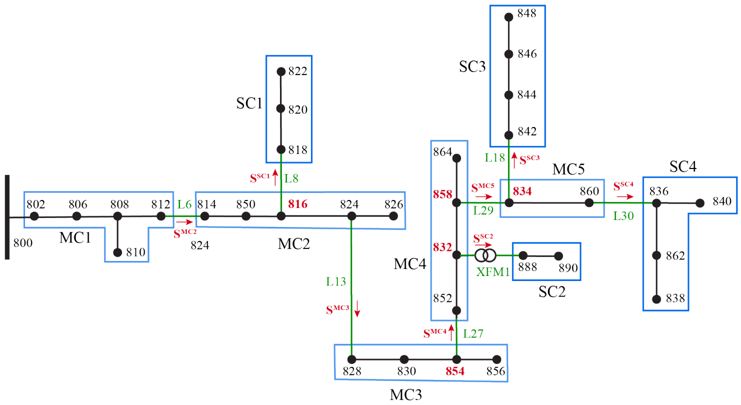

Figure 7. The CCN representation of the IEEE 34 bus system.

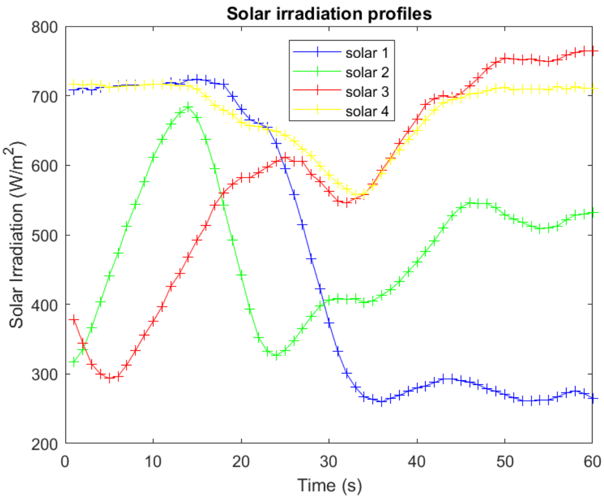

Figure 8. Solar irradiation variation across the one minute time frame of interest.

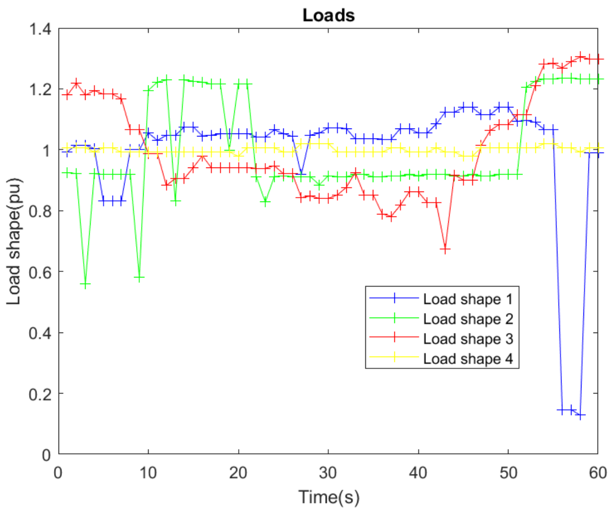

Figure 9. Load variation across the optimized one minute time frame.

5. Results and Discussion

Simulations are conducted for the two cell ranking strategies, and the results are compared with the state-of-the-art approach. Figure 10 compares the utility between CCN optimized and standard VVC across a time frame of 1 min. The utility value for the standard VVC is significantly higher than any of the two CCN optimized values across the time frame. The impact factor-based approach shows better performance when compared to the graph-based approach. The difference in performance is comparatively significant in terms of the speed of optimization based on the results shown in Tables A3 and A5. However, the impact factor calculation requires an extra step of computation, as shown in Table A4. However, the additional computation step results in the impact factor requiring four fewer steps to arrive at the utility value of 0.0218 and therefore is well justified. Figure 11 compares the corresponding mean voltage across the feeder. As expected, the mean voltage of the CCN based approach is significantly lower than the standard VVC. The calculated optimal power set-points define the operation point to which the volt-var curves are shifted. The results clearly show that the local static volt-var control is insufficient to ensure optimal operation. This is due to the nature of droop-based control, where it is impossible to address the inherent steady-state error.

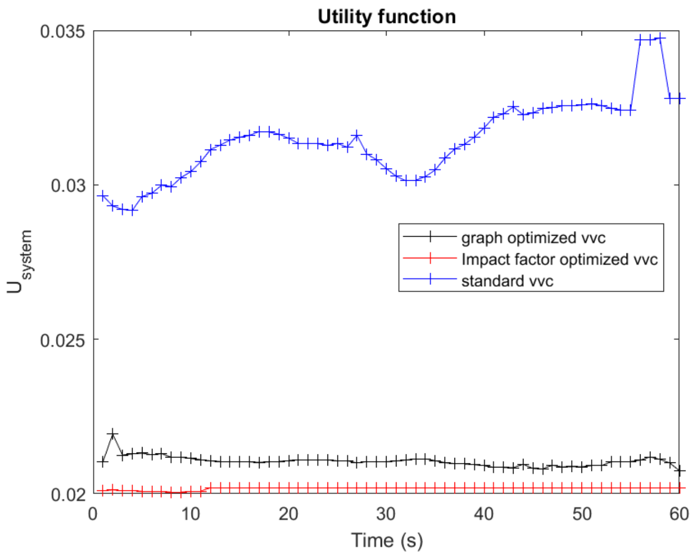

Figure 10. Comparison of utility across the optimized one minute time frame.

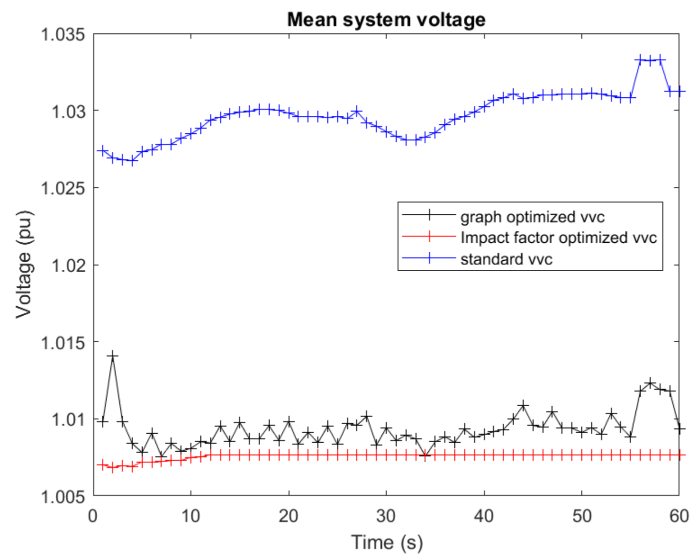

Figure 11. Comparison of voltage across the optimized one minute time frame.

Figures 8 and 9 show the source of the dynamics in the system that were applied to the loads and the PV plants. Figure 12 compares the corresponding voltages of three randomly selected nodes in the system. The voltage of the CCN based approaches is higher in quality and close to the desired value of 1 pu. Figure 13 compares the performance of the graph-based method with the impact factor-based approach. The results show that the computation time per optimized cell is comparable for both methods, whereas the utility decreases much faster for the impact factor-based approach. Therefore, the impact factor-based approach performs better than the graph-based approach.

Figure 14 compares the volt-var curves for the three operation conditions. Based on Table A5, SC3 is the first cell to be optimized in the impact-based method. From the volt-var curve, it is observed that node 844 has significant reactive power absorption in comparison to the other two methods. Since 844 is the largest DER, it is clear that cell SC3 is facing an overvoltage condition, which is compensated by selecting the volt-var curve such that SC3 is absorbing reactive power. Instead of the adaptive optimization, if standard VVC was used, the cell's potential to contribute to voltage control of the system would have been unused. Additionally, the impact factor-based approach can accelerate system optimization since it optimizes in merit order.

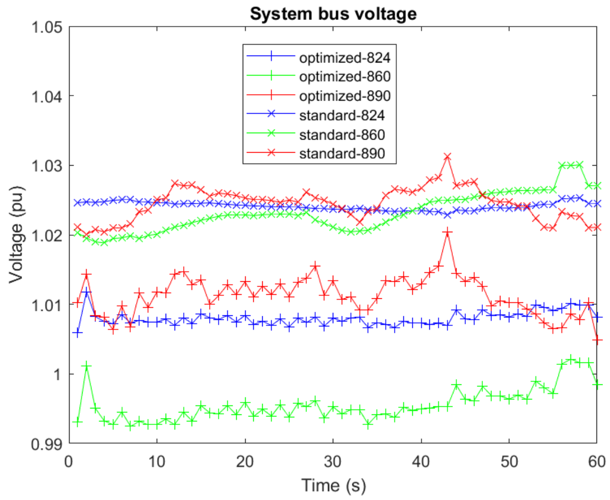

Figure 12. Comparison of voltage of three randomly selected nodes across the optimized one minute time frame.

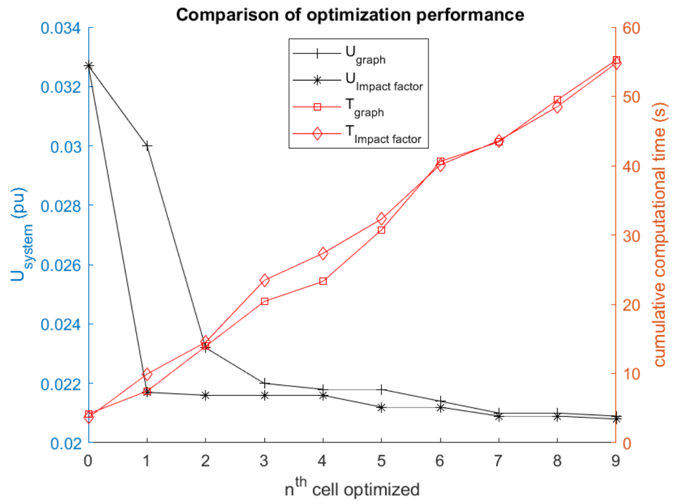

Figure 13. Comparison of optimization performance. Here, T_{graph} and $T_{impact factor}$ represents the cumulative time for each iteration, where time is given in the right y-axis, and the U_{graph} and U_{Impact_factor} gives the utility value for each iteration, where utility is shown in the left y-axis.

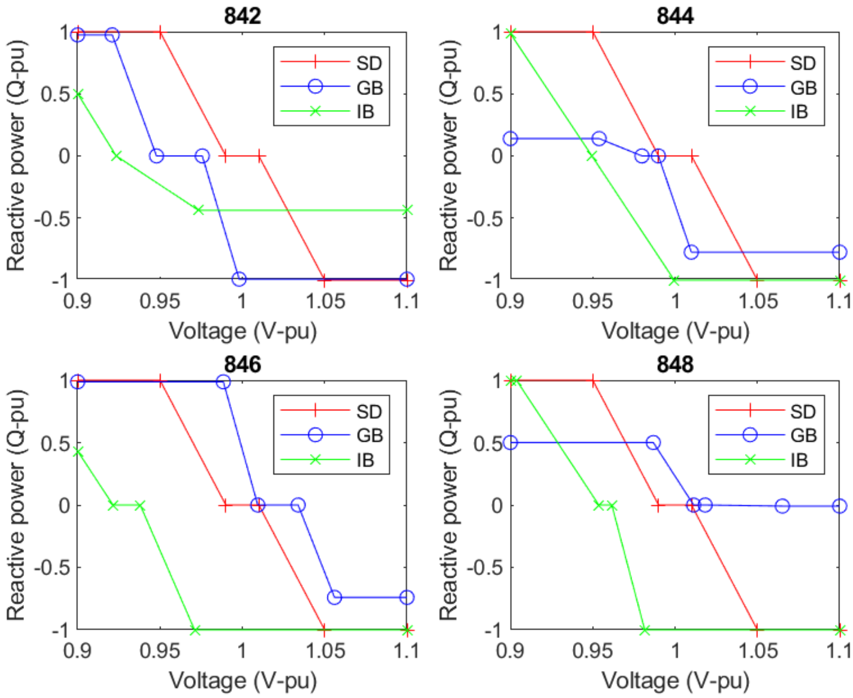

Figure 14. The volt-var curve for cell SC3.

6. Conclusions

Due to the increasing penetration of distributed energy resources (DER), voltage control in modern electric power distribution systems has become challenging. The current state-of-the-art voltage control is based on a static and pre-set DER volt-var curves and do not provide sufficient flexibility to address the dynamic aspects of the voltage control problem in a power distribution system.

This study has presented a distributed optimization framework for volt-var curves of DERS in an electric power distribution systems. The DOF is based on a cellular computational network representation of the electric power distribution system. The proposed method enhanced the system voltage control by optimizing concurrently mulitple volt-var curve parameters. The method had three functional levels, node, cell, and system. The node level used the adaptive VVC setpoints generated by the cell level. The cell level optimized the utility for the cell and generated the VVC set points for the nodes. The system-level iteratively called on cells based on the cell ranking and converged the cell parameters towards near-global optimality.

The cellular optimization approach enabled the system-wide optimization. The cell optimization was prioritized using two methods, graph and impact-based methods. The impact-based method required extra initial computational efforts but thereafter provided better computational throughput than the graph-based method. The DOF was illustrated on a modified standard distribution test case with several DERs. The results from the test case demonstrated that the DOF based volt-var optimization result in consistently better performance than the state-of-the-art volt-var control.The proposed approach needed less computation and allowed for distributed scalable optimization of a power distribution system. The presented approach will be extended with different operational scenarios and test cases, including control and hardware-in-the-loop tests and distribution systems with different characteristics. From a computational point of view, a potential future study is to extend cell DOF from sequential to parallel implementation to allow for accelerated performance.

Author Contributions: Conceptualization, H.D. and G.K.V.; methodology, H.D. and G.K.V.; software, H.D. and G.K.V.; validation, H.D. and G.K.V.; formal analysis, H.D. and G.K.V.; investigation, H.D. and G.K.V.; resources, G.K.V.; data curation, H.D.; writing—original draft preparation, H.D. and G.K.V.; writing—review and editing, H.D. and K.V; visualization, H.D. and G.K.V.; supervision, G.K.V.; project administration, G.K.V.; funding acquisition, G.K.V. All authors have read and agreed to the published version of the manuscript.

Funding: This research was funded by US NSF grants CNS 2131070 and the Duke Energy Distinguished Professor Endowment Fund.

Institutional Review Board Statement: Not applicable.

Informed Consent Statement: Not applicable.

Data Availability Statement: This study did not report any data.

Conflicts of Interest: The authors declare no conflict of interest.

Abbreviations

The following abbreviations are used in this manuscript:

VVC	Volt-Var Control
CCN	Cellular Computational Network
PV	Photo-voltaic
GB	Graph Based
IB	Impact Based
PSO	Particle Swarm Optimization
DER	Distributed Energy Resources
EPDS	Electric Power Distribution System
CR	Cell Rank

Appendix A

Table A1. Assignment of different loadshapes to power conversion components in the case study. These time variant loadshapes are the source for dynamics.

Dynamic Shape	Power Conversion Component
Solar 1	PV 802, 806, 808, 816, 824, 810, 818
Solar 2	PV 820, 822, 856, 826, 828, 830, 832
Solar 3	PV 864, 844, 848, 854, 858, 834, 836
Solar 4	PV 838, 860, 862, 840, 842, 846, 890
Load shape 1	Load 844, 802, 828, 854, 858, 836, 862
Load shape 2	Load 860, 830, 808, 824, 832, 838
Load shape 3	Load 890, 834, 836, 840, 864, 856
Load shape 4	Load 848, 806, 818, 820, 822, 816, 826

Table A2. Connected DER to the test case.

Node	Inverter Size (kVA)
802	60
806	60
808	32
810	32

Table A2. *Cont.*

Node	Inverter Size (kVA)
816	10
818	68
820	342
822	274
824	90
826	80
828	14
830	51
834	248
836	97
838	56
840	83
842	19
844	661
846	96
848	135
852	8
854	8
856	8
858	39
860	392
862	56
864	4
890	604

Table A3. Sequentially optimized utility values.

No	Cell	U.sys	Unet.MC1	Unet.MC2	Unet.MC3	Unet.MC4	Unet.MC5	Unet.SC1	Unet.SC2	Unet.SC3	Unet.SC4
NA	wo VVC	0.0720	0.0567	0.0628	0.0725	0.0791	0.0830	0.0600	0.0802	0.0834	0.0831
0	Std VVC	0.0327	0.0396	0.0291	0.0289	0.0284	0.0306	0.0247	0.0227	0.0307	0.0302
1	SC4	0.0300	0.0394	0.0284	0.0259	0.0234	0.0243	0.0246	0.0187	0.0244	0.0240
2	MC5	0.0232	0.0368	0.0217	0.0150	0.0094	0.0077	0.0186	0.0088	0.0078	0.0073
3	SC3	0.0220	0.0359	0.0192	0.0116	0.0063	0.0047	0.0163	0.0070	0.0047	0.0047
4	MC4	0.0218	0.0358	0.0187	0.0110	0.0060	0.0047	0.0159	0.0068	0.0047	0.0048
5	SC2	0.0218	0.0357	0.0186	0.0109	0.0060	0.0049	0.0158	0.0061	0.0049	0.0050
6	MC3	0.0214	0.0353	0.0173	0.0096	0.0057	0.0052	0.0147	0.0061	0.0052	0.0053
7	MC2	0.0210	0.0344	0.0151	0.0080	0.0058	0.0058	0.0136	0.0067	0.0058	0.0063
8	SC1	0.0210	0.0342	0.0144	0.0083	0.0074	0.0074	0.0101	0.0078	0.0074	0.0075
9	MC1	0.0209	0.0339	0.0142	0.0083	0.0075	0.0075	0.0099	0.0079	0.0075	0.0077

Table A4. Results from the Impact factor evaluation based on available reactive power resources and U_{sys} for cell reactive power injection.

Cell	dUsys/dQ	Q	Q.dUsys/dQ	Sequence
SC3	0.0000300	2730	0.0819	1
SC2	0.0000333	1811	0.0603	2
MC5	0.0000299	1921	0.0575	3
SC4	0.0000300	765	0.0230	4
MC2	0.0000191	541	0.0103	5
SC1	0.0000149	684	0.0102	6
MC3	0.0000239	228	0.0054	7
MC4	0.0000293	161	0.0047	8
MC1	0.0000068	555	0.0037	9

Table A5. Impact factor based priority based CCN: calculated utility function values for system and cells.

No	Cell	U.sys	Unet.MC1	Unet.MC2	Unet.MC3	Unet.MC4	Unet.MC5	Unet.SC1	Unet.SC2	Unet.SC3	Unet.SC4
0	Std VVC	0.0327	0.0396	0.0291	0.0289	0.0284	0.0306	0.0247	0.0227	0.0307	0.0302
1	SC3	0.0217	0.0355	0.0182	0.0107	0.0059	0.0047	0.0159	0.0071	0.0047	0.0051
2	SC2	0.0216	0.0354	0.0180	0.0105	0.0061	0.0048	0.0157	0.0068	0.0047	0.0051
3	MC5	0.0216	0.0355	0.0184	0.0111	0.0063	0.0045	0.0160	0.0066	0.0045	0.0046
4	SC4	0.0216	0.0356	0.0184	0.0111	0.0059	0.0037	0.0159	0.0059	0.0037	0.0035
5	MC2	0.0212	0.0347	0.0163	0.0095	0.0061	0.0047	0.0147	0.0070	0.0047	0.0050
6	SC1	0.0212	0.0346	0.0156	0.0096	0.0072	0.0061	0.0110	0.0079	0.0061	0.0061
7	MC3	0.0209	0.0341	0.0144	0.0085	0.0070	0.0062	0.0100	0.0080	0.0062	0.0062
8	MC4	0.0209	0.0342	0.0146	0.0086	0.0068	0.0059	0.0102	0.0078	0.0059	0.0060
9	MC1	0.0208	0.0339	0.0144	0.0086	0.0069	0.0062	0.0101	0.0080	0.0061	0.0062

References

1. Vaughan, A. The first global energy crisis. *New Sci.* **2022**, *253*, 18–21. [CrossRef].
2. Sioshansi, F. *Consumer, Prosumer, Prosumager: How Service Innovations Will Disrupt the Utility Business Model*; Academic Press: Cambridge, MA, USA, 2019. [CrossRef].
3. Brown, R.E. *Electric Power Distribution Reliability*, 2nd ed.; CRC Press: Boca Raton, FL, USA, 2017.
4. Rosetto, N.; Reif, V. Digitalization of the electricity infrastructure: A key enabler for the decarbonization and decentralization of the power sector. In *A Modern Guide to the Digitalization of Infrastructure*; Edward Elgar Publishing: Cheltenham, UK, 2021.
5. Roy, N.K.; Pota, H.R. Current status and issues of concern for the integration of distributed generation into electricity networks. *IEEE Syst. J.* **2015**, *9*, 933–944.
6. Turitsyn, K.; Šulc, P.; Backhaus, S.; Chertkov, M. Distributed control of reactive power flow in a radial distribution circuit with high photovoltaic penetration. In Proceedings of the IEEE PES General Meeting, Minneapolis, MN, USA, 25–29 July 2010; pp. 1–6.
7. Katiraei, F.; Agüero, J.R. Solar PV integration challenges. *IEEE Power Energy Mag.* **2011**, *9*, 62–71.
8. Kishore, P.V.; Reddy, S.R.; Kishore, P.V. Modeling and simulation of 14 bus system with D-STATCOM for powerquality improvement. *Indian J. Sci. Res.* **2012**, *3*, 73–80.
9. Moghe, R.; Tholomier, D.; Divan, D.; Schatz, J.; Lewis, D. Grid Edge Control: A new approach for volt-var optimization. In Proceedings of the 2016 IEEE/PES Transmission and Distribution Conference and Exposition (T&D), Dallas, TX, USA, 3–5 May 2016; pp. 1–5.
10. Haque, M.H. Compensation of distribution system voltage sag by DVR and D-STATCOM. In Proceedings of the Power Tech Proceedings, Manchester, UK, 18–22 June 2001; Volume 1, p. 5.
11. Karunarathne, E.; Wijethunge, A.; Ekanayake, J. Enhancing PV hosting capacity using voltage control and employing dynamic line rating. *Energies* **2021**, *15*, 134.

12. Dharmawardena, H.; Arzani, A.; Venayagamoorthy, G.K. Distributed voltage control for distribution feeder with photovoltaic systems. In Proceedings of the 2018 IEEE Power & Energy Society Innovative Smart Grid Technologies Conference (ISGT), Washington, DC, USA, 19–22 February 2018; pp. 1–8.
13. Gutierrez-Lagos, L.; Ochoa, L.F. OPF-based CVR operation in PV-rich MV–LV distribution networks. *IEEE Trans. Power Syst.* **2019**, *34*, 2778–2789.
14. Liu, M.Z.; Ochoa, L.F.; Low, S.H. On the implementation of OPF-based setpoints for active distribution networks. *IEEE Trans. Smart Grid* **2021**, *12*, 2929–2940.
15. Acosta, M.N.; Gonzalez-Longatt, F.; Andrade, M.A.; Torres, J.L.R.; Chamorro, H.R. Assessment of Daily Cost of Reactive Power Procurement by Smart Inverters. *Energies* **2021**, *14*, 4843. [CrossRef].
16. Lee, H.J.; Yoon, K.H.; Shin, J.W.; Kim, J.C.; Cho, S.M. Optimal parameters of volt–var function in smart inverters for improving system performance. *Energies* **2020**, *13*, 2294.
17. Turitsyn, K.; Sulc, P.; Backhaus, S.; Chertkov, M. Options for control of reactive power by distributed photovoltaic generators. *Proc. IEEE* **2011**, *99*, 1063–1073.
18. Photovoltaics, D.G.; Storage, E. *1547-2018—IEEE Standard for Interconnection and Interoperability of Distributed Energy Resources with Associated Electric Power Systems Interfaces*; IEEE: New Yokk, NY, USA, 2018.
19. Maknouninejad, A.; Qu, Z. Realizing unified microgrid voltage profile and loss minimization: A cooperative distributed optimization and control approach. *IEEE Trans. Smart Grid* **2014**, *5*, 1621–1630.
20. Magnússon, S.; Qu, G.; Li, N. Distributed optimal voltage control with asynchronous and delayed communication. *IEEE Trans. Smart Grid* **2020**, *11*, 3469–3482.
21. Li, N.; Qu, G.; Dahleh, M. Real-time decentralized voltage control in distribution networks. In Proceedings of the 2014 52nd Annual Allerton Conference on Communication, Control, and Computing (Allerton), Monticello, IL, USA, 30 September–3 October 2014; pp. 582–588.
22. Jafari, M.; Olowu, T.O.; Sarwat, A.I. Optimal smart inverters volt-var curve selection with a multi-objective volt-var optimization using evolutionary algorithm approach. In Proceedings of the 2018 North American Power Symposium (NAPS), Fargo, ND, USA, 9–11 September 2018; pp. 1–6.
23. Lee, H.; Kim, J.C.; Cho, S.M. Optimal volt–var curve setting of a smart inverter for improving its performance in a distribution system. *IEEE Access* **2020**, *8*, 157931–157945.
24. O'Connell, A.; Keane, A. Volt–var curves for photovoltaic inverters in distribution systems. *IET Gener. Transm. Distrib.* **2017**, *11*, 730–739.
25. Farivar, M.; Chen, L.; Low, S. Equilibrium and dynamics of local voltage control in distribution systems. In Proceedings of the 52nd IEEE Conference on Decision and Control, Firenze, Italy, 10–13 December 2013; pp. 4329–4334.
26. Dharmawardena, H.; Venayagamoorthy, G.K. A distributed data-driven modelling framework for power flow estimation in power distribution systems. *IET Energy Syst. Integr.* **2021**, *3*, 367–379.
27. Grant, L.L.; Venayagamoorthy, G.K. Cellular Multilayer Perceptron for Prediction of Voltages in a Power System. In Proceedings of the 2009 15th International Conference on Intelligent System Applications to Power Systems, Curitiba, Brazil, 8–12 November 2009; IEEE: Curitiba, Brazil, 2009; pp. 1–6. [CrossRef].
28. Luitel, B.; Venayagamoorthy, G.K. Decentralized Asynchronous Learning in Cellular Neural Networks. *IEEE Trans. Neural Netw. Learn. Syst.* **2012**, *23*, 1755–1766. [CrossRef].
29. Singh, R.; Alapatt, G.F.; Lakhtakia, A. Making solar cells a reality in every home: Opportunities and challenges for photovoltaic device design. *IEEE J. Electron Devices Soc.* **2013**, *1*, 129–144.
30. Pathiravasam, C.; Arunagirinathan, P.; Jayawardene, I.; Venayagamoorthy, G.K.; Wang, Y. Spatio-temporal distributed solar irradiance and temperature forecasting. In Proceedings of the 2020 International Joint Conference on Neural Networks (IJCNN), Glasgow, UK, 19–24 July 2020; pp. 1–8.
31. Trapero, J.R.; Kourentzes, N.; Martin, A. Short-term solar irradiation forecasting based on dynamic harmonic regression. *Energy* **2015**, *84*, 289–295.
32. Suresh, V.; Janik, P.; Rezmer, J.; Leonowicz, Z. Forecasting solar PV output using convolutional neural networks with a sliding window algorithm. *Energies* **2020**, *13*, 723.
33. Parson, O.; Fisher, G.; Hersey, A.; Batra, N.; Kelly, J.; Singh, A.; Knottenbelt, W.; Rogers, A. Dataport and NILMTK: A building data set designed for non-intrusive load monitoring. In Proceedings of the 2015 IEEE GLOBAL conference on Signal and Information Processing (Globalsip), Orlando, FL, USA, 14–16 December 2015; pp. 210–214. [CrossRef].
34. Del Valle, Y.; Venayagamoorthy, G.K.; Mohagheghi, S.; Hernandez, J.C.; Harley, R.G. Particle swarm optimization: Basic concepts, variants and applications in power systems. *IEEE Trans. Evol. Comput.* **2008**, *12*, 171–195.